

Article

A New Method for Mobility Logging Evaluation Based on Flowing Porosity in Shale Oil Reservoirs

Bo Shen ^{1,2,*}, Yunhe Tao ³, Gang Wang ⁴, Haitao Fan ⁴, Xindong Wang ⁵ and Ke Sun ⁶

¹ Key Laboratory of Exploration Technologies for Oil and Gas Resources of Ministry of Education, Yangtze University, Wuhan 430010, China

² Geophysics and Oil Resource Institute, Yangtze University, Wuhan 430010, China

³ Southwest Branch, CNPC Logging Company Limited, Chongqing 400021, China

⁴ Research Institute of Exploration and Development, Xinjiang Oilfield Company, CNPC, Karamay 834000, China

⁵ Materials and Equipment Center of CNPC Well Logging Co., Ltd., Xi'an 710200, China

⁶ Library, Yangtze University, Wuhan 430010, China

* Correspondence: shhd151@126.com; Tel.: +86-27-6911-1036

Abstract: Shale oil reservoirs differ from conventional reservoirs in several aspects, including the sedimentary model, accumulation mechanism, and reservoir characteristics, which pose significant challenges to their exploration and development. Therefore, identifying the location of optimal spots is crucial for the successful exploration and development of shale oil reservoirs. Mobility, particularly in low-permeability shale oil reservoirs with nano-scale pores, is a crucial petrophysical property that determines the development plan. However, two-dimensional nuclear magnetic resonance (2D-NMR) is expensive and has limited applicability, although it can estimate shale oil mobility. Hence, it is of great significance to find a precise method for evaluating shale oil mobility using conventional logging. In this paper, we propose a new method for assessing shale oil mobility based on free oil porosity derived from the difference in flowing porosity detected at different ranges of logging, utilizing the Maxwell conductivity model and conductivity efficiency theory. Our study shows that longitudinal-T2 (T1-T2) NMR logging can accurately evaluate the mobility of shale oil. This is demonstrated by comparing the processing results obtained from our proposed method with those from 2D-NMR and laboratory NMR experiments. The predicted results based on conventional well logs also show good agreement with experimental results, confirming the effectiveness and reliability of our new method. Our proposed method carries reference significance for evaluating shale oil reservoir quality.

Keywords: shale oil; mobility; free oil porosity; flowing porosity; conventional well logs



Citation: Shen, B.; Tao, Y.; Wang, G.; Fan, H.; Wang, X.; Sun, K. A New Method for Mobility Logging Evaluation Based on Flowing Porosity in Shale Oil Reservoirs.

Processes **2023**, *11*, 1466. <https://doi.org/10.3390/pr11051466>

Academic Editors: Liang Xiao, Xin Nie, Mehdi Ostadhassan and Hongyan Yu

Received: 6 April 2023

Revised: 7 May 2023

Accepted: 9 May 2023

Published: 11 May 2023



Copyright: © 2023 by the authors. Licensee MDPI, Basel, Switzerland. This article is an open access article distributed under the terms and conditions of the Creative Commons Attribution (CC BY) license (<https://creativecommons.org/licenses/by/4.0/>).

1. Introduction

With the continuous exploration, development, and consumption of conventional oil and gas resources, it is necessary for people to broaden their horizons and focus on more diverse energy supplies. Unconventional energy sources have gradually become an important source of global energy supply [1–13]. Unconventional reservoirs are defined by the USA Gas Policy Act of 1978 as those that exhibit a matrix permeability lower than 0.1 mD [14]. Petrophysically, their permeability is often even lower, typically less than 0.01 mD. These differences result in unconventional oil and gas reservoirs having distinct enrichment patterns, exploration and development requirements, and evaluation methods compared to conventional reservoirs. Consequently, special drilling and completion techniques, such as horizontal wells and multistage hydraulic fracturing, must be employed in unconventional reservoirs to achieve commercial hydrocarbon production [15].

Although experimental analysis can provide precise reservoir quality parameters, the cost, feasibility, and practicality of experimental methods are often limiting factors. Therefore, it is necessary to find more reasonable and feasible methods for evaluating reservoir

quality. An essential parameter in interpreting and evaluating well logs is water saturation. Hydrocarbon saturation depends on several inputs, including resistivity logs, porosity, water resistivity, and parameters obtained by calibrating against laboratory measurements using core samples. After applying an appropriate model that takes into account the specific reservoir characteristics, we can accurately define hydrocarbon saturation [16–19]. It is crucial not only to estimate the oil and gas saturation but also to determine the flow capacity of the pore fluid, as this kind of mobility can effectively characterize the recoverable reserves of oil and gas. This information is of paramount importance in evaluating oil field development. Two closely related parameters, irreducible water saturation and water saturation, can be used to analyze the mobility of hydrocarbons. The ‘movable water method’ [20] for estimating movable water saturation and oil saturation is based on this principle. The effectiveness of the method has been confirmed through actual well data processing. This approach proves particularly effective for low-resistivity oil and gas reservoirs. Formation resistivity varies across different detection ranges according to the degree of mud invasion, which, in turn, is influenced by several factors, such as mud viscosity, reservoir permeability, drilling mud quality, and effective formation porosity [21]. The hydrocarbon mobility factor (HCM) is calculated using both deep and shallow resistivity data [22]. This method determines the hydrocarbon mobility based on differences in water saturation between the original zone and the flush zone.

In addition to conventional well logs, special logging methods are increasingly being applied to estimate the quality of unconventional oil and gas reservoirs due to the growing difficulty of logging evaluation. Nuclear magnetic resonance (NMR) logging has been used since the 1960s to capture a wider range of reservoir properties [23]. Reservoir properties, such as pore structure, pore size distribution, free-flowing porosity, and hydrocarbon viscosity, can be estimated through NMR logging interpretation. As an efficient tool for reservoir characterization, NMR logging should be calibrated with laboratory measurements to define appropriate parameters for evaluating petrophysical properties [24,25]. The combination of NMR and conventional well logs can be used to quantify hydrocarbon mobility [26]. New resistivity log data can be reconstructed based on the pore size distribution and fluid type interactions from the NMR log T2 distribution to determine mobility, which is dependent on the differences between synthetic and primary resistivity logs [27].

For more complex reservoir characteristics, such as shale gas and oil, which are characterized by organic matter and rich clay minerals, the NMR log T2 spectrum distribution provides limited information [28]. Therefore, the two-dimensional NMR technique is used to isolate hydrogen-bearing components with different NMR response characteristics. The D-T2 (Diffusion-transverse) relaxation method is an effective means of assessing shale oil and gas reservoirs. However, studies have shown that it is difficult to capture diffusion coefficients in nano-porous media and distinguish kerogen signals. Therefore, the D-T2 technique is not suitable for application in shale oil reservoirs. The longitudinal-transverse relaxation (T1-T2) technique can provide better differentiation for different hydrogen-bearing phases based on the distribution characteristics of T1 and T2 or secular relaxation rate (T2S) [29,30]. These phases include residual oil, free oil, structural water, irreducible water, and free water.

Free oil porosity is considered a significant indicator of the potential for oil production in shale oil reservoirs [14,31,32]. In the case of mud intrusion, the formation can be divided into two zones—the original zone, where initial formation water is the main conductive fluid, and the flushed zone, which contains mud conductive filtrate. The substitution and displacement of different conductive fluids result in resistivity differences between the flushed zone and the original zone, which can reflect changes in the pores of conductive or non-conductive fluid. Based on this assumption, a new method for estimating free oil pores based on the difference in conductive pore space using conventional well logs has been proposed to evaluate shale oil and gas reservoir mobility. The reliability of this method has been verified through experimental NMR results and 2D-NMR logging data.

2. Background

Shale oil exploration, as exemplified by the Bakken shale oil in the Williston Basin of North America and the Barnett shale oil in the Fort Worth Basin of Texas, has continuously yielded industrial oil and gas breakthroughs. These successful explorations demonstrate the huge resource potential of shale oil, which is characterized by source-reservoir integration and in situ reservoir formation. China has abundant shale oil reserves, with significant reserves found in the Ordos Basin, Songliao Basin, Sichuan Basin, and Junggar Basin, indicating a broad prospect for exploration and development. In recent years, significant progress has been made in the Permian Lucaogou Formation in the Jimsar Sag of the Junggar Basin, where several wells have produced industrial oil, and the first shale oil production demonstration area has been established in China. Consequently, the shale oil of the Lucaogou Formation has become a research hotspot [33–38].

The Jimsar Sag is situated in the southwest of the eastern Junggar Basin in Xinjiang, covering an area of approximately 1200 km². The Middle Permian Lucaogou Formation in this sag is characterized by a wide distribution on the plane and a large longitudinal span, with a thickness generally ranging from 100–300 m. The sedimentary center is located in the southern part of the sag, where the thickness exceeds 350 m, while the northern part is thinner, usually around 100–200 m. The Lucaogou Formation belongs to fine-grained mixed sedimentary rocks. For low porosity and ultra-low permeability reservoirs like shale oil, even though the oil saturation of tight reservoirs is high due to the close proximity between source rocks and reservoirs, the nano-scale pore throat system in the reservoir is dominant, and the oil quality is heavy. This results in low mobility of shale oil [39–44]. While NMR logging has some advantages in evaluating shale oil mobility, its high cost makes it impractical to use on a wide scale. Therefore, there is a need to propose a method for estimating shale oil mobility based on conventional logging data.

3. Methods

3.1. Flowing Porosity Obtained by Core Samples

In the study of logging evaluation for any type of reservoir, the formation factor of porous media is a crucial indicator. This concept is not only one of the essential factors for evaluating hydrocarbon saturation using logging but also the key parameter for the tortuosity evaluation model, which refers to the flowing path through porous rocks [45–48]. The Archie equation [16] is the most commonly used formula for describing the formation factor and rock porosity. The general form of this equation can be expressed as follows:

$$F = \frac{R_o}{R_w} = \frac{a}{\varphi^m} \quad (1)$$

where F refers to the formation factor, which is a unitless parameter. R_w represents the resistivity of the conductive fluid occupying the porous medium, expressed in ohm-m. R_o denotes the rock sample resistivity when it is saturated with conductive fluid (brine), also expressed in ohm-m. Winsauer et al. [45] introduced the lithology coefficient “ a ” to account for the non-zero offset. For a given porous rock, “ a ” and “ m ” are inherent properties that depend closely on its lithology, cement composition, and content. Both “ a ” and “ m ” are unitless parameters.

Theoretically, a simple assumption is that discontinuously dispersed spheres act as non-conductive materials in a conductive medium, such as initial formation water. This hypothesis was first proposed by the physicist Maxwell [49]. The relationship between porosity and formation factor can be expressed as follows:

$$F = 1 + 1.5(\varphi^{-1} - 1) \quad (2)$$

where φ is the rock porosity in fraction.

Under reservoir conditions, rock matrix grains represent a discontinuously dispersed non-conductive medium. The connected pore space containing the initial formation water is a conductive medium (as shown in Figure 1). When an electric current flows through the initial formation water, it encounters resistance as it passes through the non-conductive rock matrix grains. The path of the electric current will change as it bypasses the rock matrix grains because of the difference in the degree of cementation of rock matrix grains and the reason for the instantaneous current direction change when the current encounters the non-conductive medium of the sphere. As a result, there is still “current trapping space” in the continuous conductive pore fluid (the black around T indicates the pore space without current). Even if the connected pores are completely saturated with initial formation water, there is still no flowing electric current in some connected pores, which does not contribute to the conductive network.

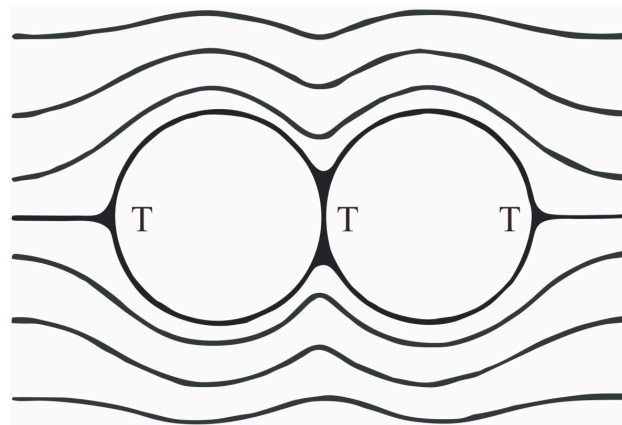


Figure 1. Electric current and trap regions (T area) around non-conductive rock matrix grains.

Equation (2) involves many assumptions, and its conclusions are derived under ideal conditions, making it less directly applicable in evaluating reservoirs using well logs. To expand the applicability of the Maxwell model, a geometrical parameter [50] was introduced into the equation. When we assume an ellipsoid to be a non-conductive medium in the conducting system, the formation factor can be expressed as follows:

$$F = 1 + (1 + x^{-1})(\varphi^{-1} - 1) \quad (3)$$

where x is a unitless geometrical parameter that represents the ratio of the long and short axes of the non-conductive ellipsoid. When x equals 2, Equation (2) simplifies to Equation (1), with the insulating medium changing from an ellipsoid to a sphere. In most cases, however, x is less than 2.

Figure 2 illustrates a schematic diagram of trapped and conductive pore spaces in porous rock. Due to the complexity of the connected pore space network, even when the rock sample is fully saturated with conductive initial formation water, some “T” zones still trap electric current and are unable to contribute to the conductive network of the pore space. In other words, only the connected pore spaces marked as “C” truly participate in the conduction mechanism. From the perspective of the electric current migration capacity of the conductive fluid in the connected pore space, total porosity can be decomposed into static and flowing porosity, which can be expressed by the following formula:

$$\varphi = \varphi_f + \varphi_s \quad (4)$$

where φ_f is flowing porosity and φ_s is static porosity, and the units of them are fractions.

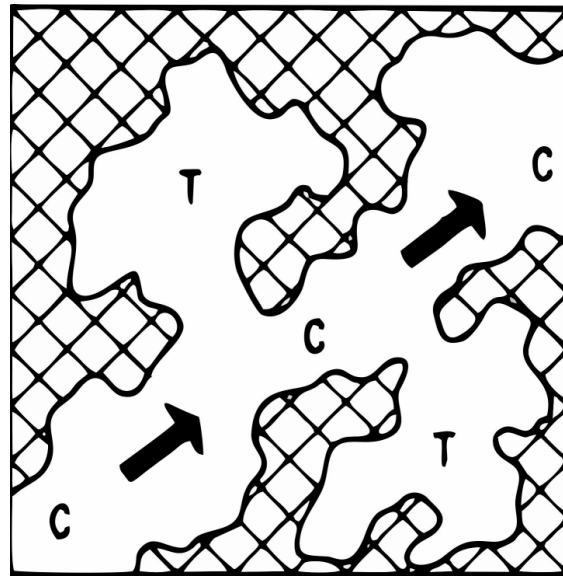


Figure 2. The trapped and conductive pore space of porous rock.

Using the research findings of Fricke and Maxwell, the relationship between the formation factor and total porosity can be transformed into a relationship between the formation factor and flowing porosity based on the differences in pore space within the actual conductive network. As a result, Equation (3) can be expressed in a modified form [51]:

$$F = 1 + (1 + x^{-1})(\varphi_f^{-1} - 1) \quad (5)$$

Based on the theoretical analysis and formula derivation presented above, x can only serve as an indicator of the non-conductive medium's geometry factor (rock matrix grains) when all connected pore spaces are fully saturated with conductive initial formation water and have a flowing electric current. In cases where the pore structure remains unchanged, x represents the geometry of the non-conductive rock matrix grains when the pore space is fully saturated with conductive initial formation water. Due to the difference between the porosity that actually participates in the current conduction contribution and the total porosity, the geometric parameter x in Equation (5) is replaced by the flowing geometric parameter x_f . The difference between x and x_f is essential because the flowing porosity is not equal to the total porosity. Equation (3) represents the formula under ideal conditions where the flowing porosity is the same as the total porosity. However, in reality, the flowing porosity is often smaller than the total porosity, resulting in x_f being greater than x . Therefore, a further modified version of Equation (5) can be expressed as a relationship between the flowing geometry parameter and flowing porosity to characterize the formation factor:

$$F = 1 + (1 + x_f^{-1})(\varphi_f^{-1} - 1) \quad (6)$$

where x_f is the flowing geometry factor and is unitless.

3.2. Establishment of Flowing Porosity Model

The primary lithogenic minerals, such as quartz, feldspar, and carbonates, are almost non-conductive materials, and changes in resistivity-logging data are primarily caused by differences in initial formation water saturation within connected pore spaces. However, actual factors influencing resistivity logging are far more complex than initially expected. Apart from conductive minerals, shale volume content, pore structure, wettability, and other internal reservoir factors also affect resistivity logging. Additionally, external factors, such as mud properties and wellbore conditions, can also influence resistivity logging. Thus, resistivity logging can be measured within a certain range even in tight reservoirs with

very low porosity. Resistivity logging is a comprehensive response to lithology, porosity, permeability, hydrocarbon saturation, and other reservoir characteristics. It is challenging to differentiate the response characteristics of individual factors from resistivity logging. In practice, the resistivity of the rock matrix is typically represented by a constant or a function of water saturation [52].

In this paper, we propose a method for determining flowing porosity. First, we define background conductivity (C_{bg}) as the conductivity under the combined influence of various coupling factors. In the original zone, if the flow porosity is zero, meaning there is no free-flowing electric current in the connected pore space, then the conductivity measured by resistivity logging (C_t) equals the background conductivity (C_{bg}). Conversely, when the flowing porosity is equal to 1, and there is no trapped electric current, the conductivity measured by resistivity logging (C_t) represents the conductivity of the pore fluid (C_f).

Taking into account the aforementioned conductivity boundary limitations, and based on the linear superposition property of conductivity, the flowing porosity can be expressed as follows:

$$\varphi_f = \frac{C_t - C_{bg}}{C_f - C_{bg}} \quad (7)$$

where C_{bg} , C_t , and C_f represent the background conductivity, conductivity, and pore fluid conductivity of the original zone, respectively, with a unit of S/m.

Based on the above analysis of conductive mechanisms using the theories of flowing porosity and static porosity, it is apparent that there exist some connected pore spaces in rock samples saturated with an initial formation water that does not contribute to conductivity due to factors such as pore structure and distribution characteristics. Therefore, the water-filled porosity (φ_w) and flowing porosity (φ_f) are not equal. When oil–water two-phase fluids coexist, the conductivity of the pore fluid is mainly influenced by the flowing porosity filled with free electric current and the properties of the formation water. Since hydrocarbons are non-conductive fluids, the conductivity of the pore fluid can be calculated using the following formula:

$$C_f = \frac{\varphi_f}{\varphi} C_w = S_{wf} C_w \quad (8)$$

where C_w represents the conductivity of water in rock pores measured in S/m (Siemens per meter) and S_{wf} represents the fraction of conductive water saturation.

According to Equations (7) and (8), if there is no electric current in the connected pore space, the flowing porosity (φ_f) is equal to 0, the total porosity (φ) is equal to the static porosity (φ_s), and the conductivity obtained from resistivity logging equals the background conductivity. On the other hand, when the flowing porosity (φ_f) is equal to 1 and the static porosity (φ_s) is equal to 0, the measured conductivity acquired from resistivity logging represents the conductivity of the initial formation water. Equation (7) is revised as follows:

$$\frac{\varphi_f}{\sigma} = \frac{C_t - C_{bg}}{C_f - C_{bg}} \quad (9)$$

where σ is a dimensionless structural indicator that represents the connected pore space in the original zone and distinguishes it from the total pore space. By combining Equations (8) and (9), the flowing porosity can be determined using the following equation:

$$C_w \varphi_f^2 - C_{bg} \varphi \varphi_f - \sigma (C_t - C_{bg}) \varphi = 0 \quad (10)$$

The positive solution of the quadratic equation represents the value of the flowing porosity. According to Equation (10), if the flowing porosity (φ_f) is equal to 0, the background conductivity of the original zone (C_{bg}) equals the conductivity of the original zone (C_t). In this case, the maximum resistivity logging value corresponds to the background

resistivity. On the other hand, when the flowing porosity (φ_f) equals the total porosity (φ), σ can be calculated using the following equation:

$$\sigma = \frac{(C_w - C_{bg})\varphi}{C_t - C_{bg}} \quad (11)$$

Thus, an apparent structural indicator curve can be obtained by utilizing the parameters σ and C_{bg} , which interact with each other and can adjust the results accordingly. Any issues with inappropriate C_{bg} values can be compensated for by adjusting the value of α .

3.3. Flowing Porosity Model of Flushed Zone

Assuming that other petrophysical and geophysical characteristics remain constant, changes in flowing porosity indicate differences in the conductive pore space filled with a free electric current in the original formation. In a flushed zone, there exists a flowing porosity as well, but the conductive fluid is no longer initial formation water; instead, it is replaced by mud filtrate. The injected mud during drilling generates high pressure to balance the formation pressure and prevent accidents such as well kicks and blowouts. In permeable reservoirs, the mud filtrate can exchange with the initial formation water. Due to factors such as pore structure, micro-pore and throat size, and wettability, residual hydrocarbons and bound formation water may be present in the pore space of the flushed zone, but these fluids are mostly trapped due to the limited pore space available for their existence. In the flushed zone, mud filtrate is the conductive fluid in the pore space. Therefore, the flowing porosity and structural indicator of the flushed zone can be obtained using Equations (10) and (11), and the two parameters can be expressed as follows:

$$\sigma_{xo} = \frac{(C_{mf} - C_{bgxo})\varphi}{C_{xo} - C_{bgxo}} \quad (12)$$

$$C_{mf}\varphi_{fxo}^2 - C_{bgxo}\varphi\varphi_{fxo} - \sigma_{xo}(C_{xo} - C_{bgxo})\varphi = 0 \quad (13)$$

where, C_{mf} , C_{bgxo} , and C_{xo} are the respective conductivities of mud filtrate, background conductivity of the flushed zone, and mud filtrate conductivity with units of S/m. σ_{xo} is the unitless structural indicator of the flushed zone.

3.4. Free Oil Porosity (FOP)

During drilling, mud is likely to permeate into porous reservoirs and cause variations in the resistivity of the formation, which occurs due to differences between the resistivity of mud filtrate and that of the formation water. Prior to the development of the mud cake, several factors such as porosity, permeability, the pressure differential between the mud and formation, mud properties, and drilling time can impact this seepage effect. During mud filtrate invasion, the free oil pore space is gradually replaced by mud filtrate, and as a result, the conductive fluid pore space also changes. The porosity of the free oil can be determined by calculating the difference between the conductive pore space of the flushed zone and that of the original formation.

$$\text{FOP} = \varphi_{fxo} - \varphi_f \quad (14)$$

where FOP is free oil porosity, %.

Figure 3 displays a flowchart for estimating the free oil porosity using different data such as background conductivity, porosity, water conductivity, and structural indicators. By comparing the difference in flowing porosity values between the original and flushed zones, the free oil porosity of shale oil reservoirs can be obtained based on conventional well logs.

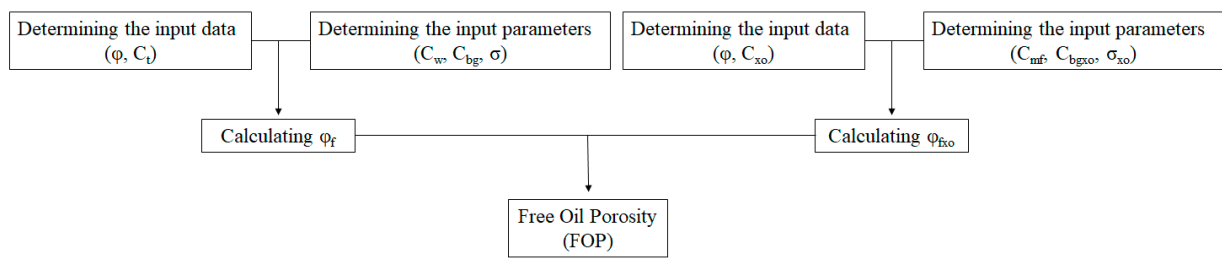


Figure 3. The flowchart for estimation of free oil porosity.

4. Results and Discussions

Figure 4 shows comparisons of free oil porosity obtained through various methods and experiments. Track 1 displays the GR, SP, and CALI logs. Track 2 exhibits the measured depth, while track 3 presents the DEN, CNL, and AC logs. The RT, RI, and RXO logs are displayed in track 4. These four tracks correspond to conventional well-logging curves that are used for identifying lithology, distinguishing effective reservoirs, determining porosity, and calculating saturation. The flowing porosities for the original and flushed zones, which were determined using the method proposed in this paper, can be found in track 5. Track 6 presents two free oil porosity curves, one obtained through conventional well logging (FOP_C) and the other acquired using NMR logging (FOP_NMRT1T2). In the last two tracks, these curves are compared with laboratory NMR experiment results. Analysis of the processing results from well J116 indicates that the variations in free oil porosity obtained through nuclear magnetic logging and conventional logging are generally consistent. Moreover, both methods exhibit good agreement with the experimentally determined free oil porosity. These findings suggest that both NMR and conventional logging are effective ways to estimate free oil porosity in shale oil reservoirs. However, the free oil porosity calculated by conventional logging displays significant variations due to resistivity changes in the flushed zone. In contrast, the free oil porosity predicted by NMR (T1-T2) logging is much smoother. The close similarity between the calculated free oil porosity and the core-analyzed values confirms the reliability of the method proposed in this paper.

Figure 5 displays the application of the proposed method, based on conventional well logs, to another well. All tracks have the same physical significance as in Figure 4. In the last track, the calculated free oil porosity obtained through the proposed method is compared with the core-derived free oil porosity. Similar to the processing results of well J116, both free oil porosity curves obtained by conventional logging and NMR (T1-T2) logging exhibit good agreement with experimental results. This indicates that the proposed method can effectively estimate free oil porosity in shale oil reservoirs. At a depth of 3026.61 m, the experimental value of free oil porosity was determined to be 1.55%. However, the interpretation result from NMR (T1-T2) logging is almost zero, while the free oil porosity calculated through conventional logging is 1.46%, indicating that for some formations, the free oil porosity obtained through conventional logging may be more reasonable. This could be attributed to the fact that when using NMR (T1-T2) logging to evaluate shale oil mobility, it is essential to calibrate the distribution characteristics of fluid occurrence states by conducting numerous effective experiments to determine the mobility characteristics of samples. Therefore, when the number of experiment samples is limited or the experimental results are poor, multiple interpretations of the results from NMR (T1-T2) logging are possible.

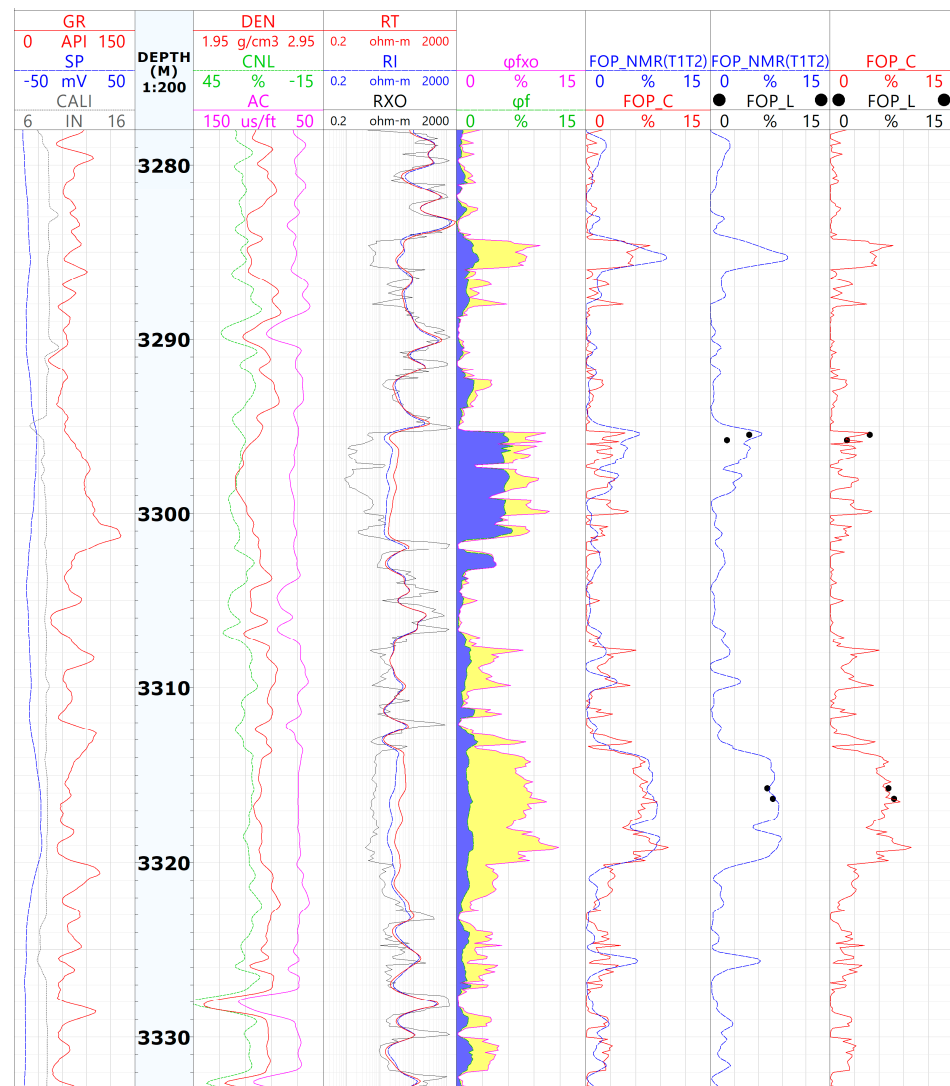


Figure 4. Comparisons of free oil porosity obtained by well logs and experiment (well J116).

Figure 6 presents a comparison between the predicted free oil porosity and core-derived free oil porosity in shale oil reservoirs of the target formation. The two porosity values show good agreement with each other. Table 1 provides a summary of the statistical analysis obtained by comparing the predicted results with laboratory NMR experiment results of 13 core samples from five wells. This table includes the coefficient of determination (R^2), average absolute error, and root mean square error (RMSE). The results indicate high R^2 values and low errors, demonstrating the accuracy of the proposed method in estimating shale oil mobility.

Table 1. The summary of statistical parameters from comparing the predicted results with the experiment results.

Criteria	FOP_C	FOP_L
Coefficient of determination	0.774	0.773
Average absolute error	1.06	1.12
Root mean square error	1.43	1.54

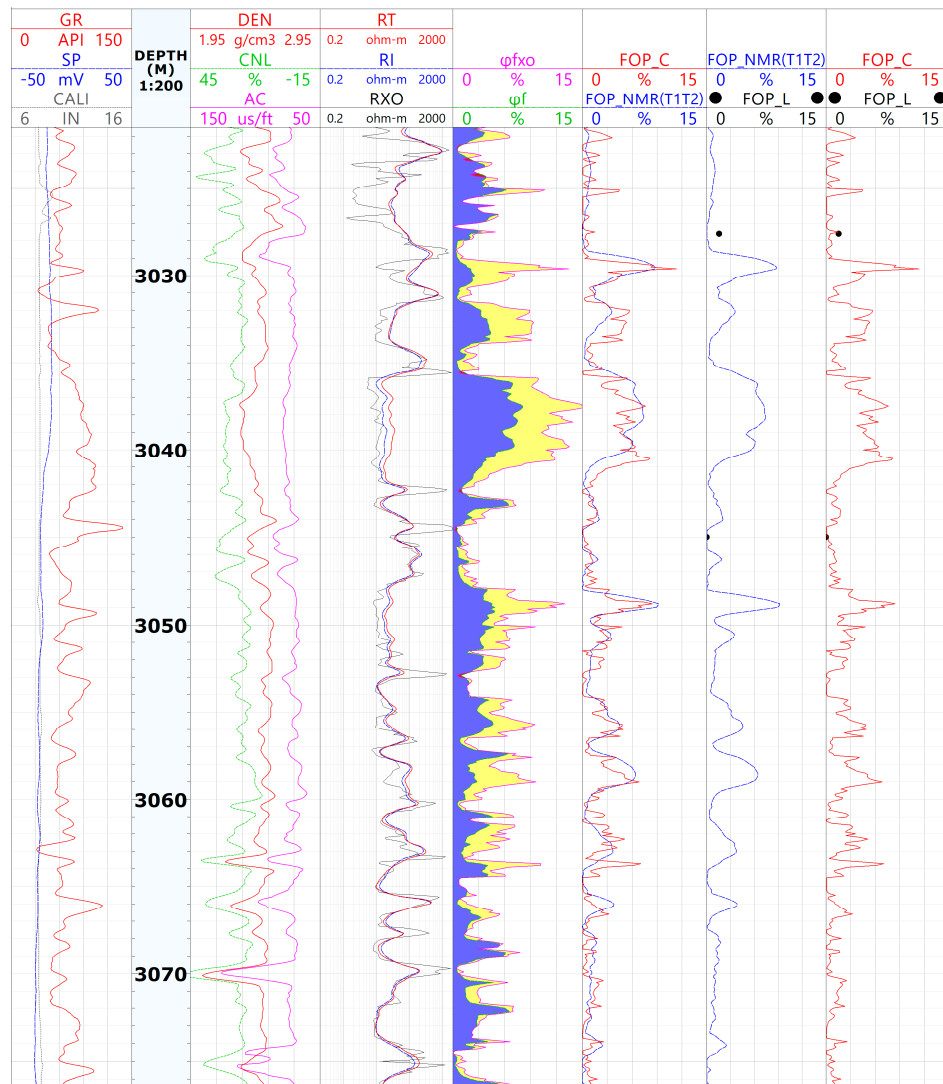


Figure 5. Comparisons of free oil porosity obtained by well logs and experiment (well J176).

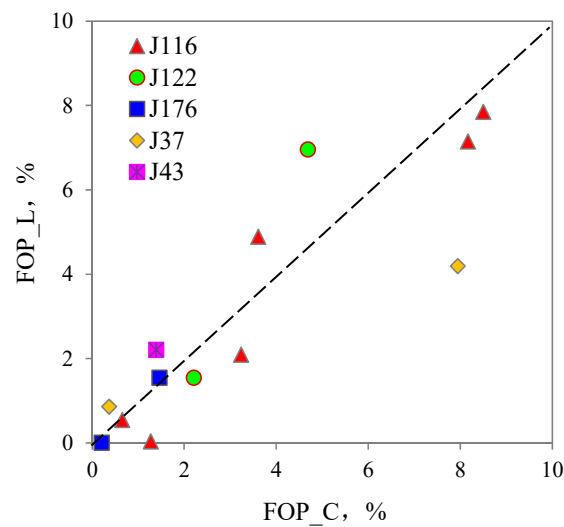


Figure 6. Comparison of predicted and core-derived free oil porosity in the shale oil reservoirs of the Permian Lucaogou Formation.

5. Conclusions

Shale oil reservoirs are typically classified as self-generating and self-storing rock reservoirs. As a result, most of the oil produced is retained in situ within nano-scale pores. The level of mobility in such reservoirs plays a crucial role in determining the success of their development. While NMR logging has been shown to be effective in assessing mobility, there are still some technical deficiencies associated with its applying. To address this concern, this paper proposes an alternative approach for estimating shale oil reservoir mobility using conventional well logs due to the limitations of NMR (T1-T2) logging and laboratory NMR experiments. According to the Maxwell model and the theory of conductivity efficiency, a method has been proposed to determine flowing porosity in shale oil reservoirs. The intrusion of mud can generally reflect changes in conductive fluid space and define shale oil mobility based on free oil porosity. Therefore, a new method for predicting free oil porosity has been established by comparing the difference in flowing porosity between the flushed zone and original zone.

The results obtained from NMR (T1-T2) logging and laboratory NMR experiments showed that the proposed method is reliable and effective for evaluating shale oil mobility. This method can be used accurately to assess the mobility of shale oil reservoirs and to predict the distribution of free oil porosity.

Author Contributions: Conceptualization, B.S.; Methodology, B.S.; Investigation, Y.T., G.W., H.F. and X.W.; Writing—Original Draft Preparation, B.S.; Writing—Review and Editing, B.S. and K.S. All authors have read and agreed to the published version of the manuscript.

Funding: This research was funded by the National Natural Science Foundation of China (Grant No. 41504103).

Data Availability Statement: The data presented in this study are available on request from the corresponding author.

Acknowledgments: The authors wish to thank the CNPC Logging Company, Core Library, for giving us access to the core samples.

Conflicts of Interest: The authors declare no conflict of interest.

References

1. Daniel, A.; Brain, B.; Bobbi, J.C. Evaluation implication of hydraulic fracturing in shale gas reservoirs. In Proceedings of the SPE Americas E & P Environmental and Safety Conference, San Antonio, TX, USA, 23–25 March 2009.
2. Sonnenberg, S.A.; Pramudito, A. Petroleum geology of the giant Elm coulee field, williston basin. *AAPG Bull.* **2009**, *93*, 1127–1153. [[CrossRef](#)]
3. Aguilera, R.F.; Radetzki, M. Shale gas and oil: Fundamentally changing global energy markets. *Oil Gas J.* **2013**, *111*, 54–60.
4. Emmanuel, O.O.; Sonnenberg, S.A. Geologic characterization and the depositional environment of the middle Devonian Marcellus shale, Appalachian Basin, NE USA. In Proceedings of the Unconventional Resources Technology Conference, Denver, CO, USA, 12–14 August 2013.
5. Romero-Sarmiento, M.F.; Ducros, M.; Carpentier, B.; Lorant, F.; Cacas, M.C.; Pegaz-Fiornet, S.; Wolf, S.; Rohais, S.; Moretti, I. Quantitative evaluation of TOC, organic porosity and gas retention distribution in a gas shale play using petroleum system modeling: Application to the Mississippiian Barnett shale. *Mar. Pet. Geol.* **2013**, *45*, 315–330. [[CrossRef](#)]
6. Guo, X.S. *The Enrichment Mechanism and Exploration Technology of Fuling Shale Gas Fields*; Science Press: Beijing, China, 2014.
7. Zhao, P.; Zhuang, W.; Sun, Z.; Wang, Z.; Luo, X.; Mao, Z.; Tong, Z. Methods for estimating petrophysical parameters from well logs in tight oil reservoirs: A case study. *J. Geophys. Eng.* **2016**, *13*, 78–85. [[CrossRef](#)]
8. Tang, H.; Sun, Z.; He, Y.; Chai, Z.; Hasan, A.R.; Killough, J. Investigating the pre unconventional gas reservoirs. *J. Pet. Sci. Eng.* **2019**, *176*, 456–465. [[CrossRef](#)]
9. Zhao, P.; Ostadhassan, M.; Shen, B.; Liu, W.; Abarghani, A.; Liu, K.; Luo, M.; Cai, J. Estimating thermal maturity of organic-rich shale from well logs: Case studies of two shale plays. *Fuel* **2019**, *235*, 1195–1206. [[CrossRef](#)]
10. Wu, Y.; Tahmasebi, P.; Yu, H.; Lin, C.; Wu, H.; Dong, C. Pore-Scale 3D Dynamic Modeling and Characterization of Shale Samples: Considering the Effects of Thermal Maturation. *JGR-Solid Earth* **2020**, *125*, e2019JB018309. [[CrossRef](#)]
11. Bai, L.H.; Liu, B.; Du, Y.J.; Wang, B.Y.; Tian, S.S.; Wang, L.; Xue, Z.Q. Distribution characteristics and oil mobility thresholds in lacustrine shale reservoir: Insights from N₂ adsorption experiments on samples prior to and following hydrocarbon extraction. *Pet. Sci.* **2022**, *19*, 486–497. [[CrossRef](#)]

12. Wang, F.Y.; Wang, L. Pore structure analysis and permeability prediction of shale oil reservoirs with HPMI and NMR: A case study of the Permian Lucaogou Formation in the Jimsar Sag, Junggar Basin, NW China. *J. Pet. Sci. Eng.* **2022**, *214*, 110503. [[CrossRef](#)]
13. Li, C.L.; Yan, W.L.; Wu, H.L.; Tian, H.; Zheng, J.D.; Yu, J.; Feng, Z.; Xu, H.J. Calculation of oil saturation in clay-rich shale reservoirs: A case study of Qing 1 Member of Cretaceous Qingshankou Formation in Gulong Sag, Songliao Basin, NE China. *Pet. Explor. Dev.* **2022**, *49*, 1351–1363. [[CrossRef](#)]
14. Piedrahita, J.; Aguilera, R. Geochemical Productivity Index (Igp): An Innovative Way to Identify Potential Zones with Moveable Oil in Shale Reservoirs. In Proceedings of the SPE Annual Technical Conference and Exhibition, Dallas, TX, USA, 24–26 September 2018.
15. Ahmed, U.; Meehan, D. *Unconventional Oil and Gas Resources Exploitation and Development*; CRC Press Taylor & Francis Group: Boca Raton, FL, USA, 2016.
16. Archie, G.E. The electrical resistivity log as an aid in determining some reservoir characteristics. *Trans. AIME* **1942**, *146*, 54–67. [[CrossRef](#)]
17. Archie, G.E. Classification of carbonate reservoir rocks and petrophysical considerations. *Am. Assoc. Petrol. Geo. Bull.* **1952**, *36*, 278–298.
18. Waxman, M.H.; Smits, L.J.M. Electrical conductivities in oil-bearing shaly sands. *Soc. Petrol. Eng. J.* **1968**, *8*, 107–122. [[CrossRef](#)]
19. Clavier, C.; Coates, G.; Dumanoir, J. Theoretical and experimental bases for the dual-water model for interpretation of shaly sands. *Soc. Petrol. Eng. J.* **1984**, *24*, 153–168. [[CrossRef](#)]
20. Zeng, W. An Effective Log Analysis for Hydrocarbon Evaluation The Movable-water Method. *Log Anal.* **1981**, *22*, 3–13.
21. Woodhouse, R. Accurate reservoir water saturation from oil-mud cores-questions and answers from Prudhoe Bay and Behind. *Log. Anal.* **1996**, *39*, 23–47.
22. Hamada, G.M. Identification of Hydrocarbon Mobility and Type from Resistivity Logs. *Pet. Sci. Technol.* **2008**, *26*, 638–648. [[CrossRef](#)]
23. Brown, R.; Gamson, B. Nuclear magnetism logging. *J. Pet. Technol.* **1960**, *12*, 199–207. [[CrossRef](#)]
24. Vincent, B.; Fleury, M.; Santerre, Y.; Brigaud, B. NMR relaxation of neritic carbonates: An integrated petrophysical and petrographical approach. *Appl. Geophys.* **2011**, *74*, 38–58. [[CrossRef](#)]
25. Souza, A.; Carneiro, G.; Zielinski, L.; Polinski, R.; Schwartz, L.; Hürlimann, M.D.; Boyd, A.; Rios, E.D.; Santos, B.C.C.; Trevizan, W.A.; et al. Permeability Prediction Improvement Using 2D NWR Diffusion-T2 Maps. In Proceedings of the SPWLA 54th Annual Logging Symposium, New Orleans, LA, USA, 22–26 June 2013.
26. Mohammadlou, M.H.; Langeland, H.; Mørk, M.B. Use of the NMR and Resistivity Logs to Quantify Movable Hydrocarbon; Solution for the Tight and Low-Resistivity Carbonate Reservoirs. In Proceedings of the Paper presented at the SPE EUROPEC/EAGE Annual Conference and Exhibition, Vienna, Austria, 23–26 May 2011.
27. Zhang, P.; Lu, S.; Li, J.; Chang, X. 1D and 2D Nuclear magnetic resonance (NMR) relaxation behaviors of protons in clay, kerogen and oil-bearing shale rocks. *Mar. Pet. Geol.* **2020**, *114*, 104210–104222. [[CrossRef](#)]
28. Birdwell, J.E.; Washburn, K.E. Multivariate analysis relating oil shale geochemical. *Energy Fuels* **2015**, *29*, 2234–2243. [[CrossRef](#)]
29. Fleury, M.; Kohler, E.; Norrant, F.; Gautier, S.; M'Hamdi, J.; Barre, L. Characterization and quantification in smectites with low field NMR. *J. Phys. Chem. C* **2013**, *117*, 4551–4560. [[CrossRef](#)]
30. Jiang, F.; Zhang, C.; Wang, K.; Zhao, Z.; Zhong, K. Characteristics of micropores, pore throats, and movable fluids in the tight sandstone oil reservoirs of the Yanchang Formation in the southwestern Ordos Basin, China. *AAPG Bull.* **2019**, *103*, 2835–2859. [[CrossRef](#)]
31. Shen, B.; Wu, D.; Wang, Z. A new method for permeability estimation from conventional well logs in glutenite reservoirs. *J. Geophys. Eng.* **2017**, *14*, 1268–1274. [[CrossRef](#)]
32. Wang, M.; Liu, M.; Li, J.B.; Xu, L.; Zhang, J.X. The key parameter of shale oil resource evaluation: Oil content. *Pet. Sci.* **2022**, *19*, 1443–1459. [[CrossRef](#)]
33. Ding, X.; Qu, J.; Imin, A.; Zha, M.; Su, Y.; Jiang, Z.; Jiang, H. Organic matter origin and accumulation in tuaceous shale of the lower Permian Lucaogou Formation, Jimsar Sag. *J. Petrol. Sci. Eng.* **2019**, *179*, 696–706. [[CrossRef](#)]
34. Jiang, Y.; Hou, D.; Li, H. Impact of the paleoclimate, paleoenvironment, and algae bloom: Organic matter accumulation in the lacustrine Lucaogou formation of jimsar sag, Junggar Basin, NW China. *Energies* **2020**, *13*, 1488. [[CrossRef](#)]
35. Jia, C.Z.; Pang, X.Q.; Song, Y. Whole petroleum system and ordered distribution pattern of conventional and unconventional oil and gas reservoirs. *Pet. Sci.* **2023**, *20*, 1–19. [[CrossRef](#)]
36. Xi, K.L.; Zhang, Y.Y.; Cao, Y.C.; Gong, J.F.; Li, K.; Lin, M.R. Control of micro-wettability of pore-throat on shale oil occurrence: A case study of laminated shale of Permian Lucaogou Formation in Jimusar Sag, Junggar Basin, NW China. *Pet. Explor. Dev.* **2023**, *50*, 334–345. [[CrossRef](#)]
37. Chen, Y.E.; Li, L.L.; Zhang, Z.R.; Paul, F.; Liu, Y.M. Biodegradation of occluded hydrocarbons and kerogen macromolecules of the Permian Lucaogou shales, Junggar Basin, NW China. *Energy Geosci.* **2023**, *4*, 179–184. [[CrossRef](#)]
38. Liu, S.J.; Gao, G.; Gang, W.Z.; Xiang, B.L.; Wang, M. Differences in geochemistry and hydrocarbon generation of source-rock samples dominated by telalginite and lamalginite: A case study on the Permian saline lacustrine source rocks in the Jimusaer Sag, NW China. *Pet. Sci.* **2023**, *20*, 141–160. [[CrossRef](#)]
39. Su, Y.; Zha, M.; Ding, X.; Qu, J.; Wang, X.; Yang, C.; Iglauer, S. Pore type and pore size distribution of tight reservoirs in the Permian Lucaogou Formation of the Jimsar sag, Junggar basin, NW China. *Mar. Petrol. Geol.* **2018**, *89*, 761–774. [[CrossRef](#)]

40. Qu, C.S.; Qiu, L.W.; Yang, Y.C.; Yang, Y.Q.; Yu, K.H. Sedimentary environment and the controlling factors of organic-rich rocks in the Lucaogou formation of the Jimusar sag, Junggar Basin, NW China. *Petrol. Sci.* **2019**, *16*, 763–775. [[CrossRef](#)]
41. Sun, L.; Zou, C.; Jia, A.; Wei, Y.; Zhu, R.; Wu, S.; Guo, Z. Development characteristics and orientation of tight oil and gas in China. *Petrol. Explor. Dev.* **2019**, *46*, 1073–1087. [[CrossRef](#)]
42. Zha, M.; Wang, S.; Ding, X.; Feng, Q.; Xue, H.; Su, Y. Tight oil accumulation mechanisms of the Lucaogou Formation in the Jimusar Sag, NW China: Insights from pore network modeling and physical experiments. *J. Asian Earth Sci.* **2019**, *178*, 204–215. [[CrossRef](#)]
43. Wang, J.; Zhou, L.; Liu, J.; Zhang, X.; Zhang, F.; Zhang, B. Acid-base alternation diagenesis and its influence on shale reservoirs in the Permian Lucaogou formation, Jimusar sag, Junggar Basin, NW China. *Petrol. Explor. Dev.* **2020**, *47*, 962–976. [[CrossRef](#)]
44. Zou, C.; Qiu, Z. Preface: New advances in unconventional Petroleum Sedimentology in China. *Acta Sedimentol. Sin.* **2021**, *39*, 1–8.
45. Winsauer, W.O.; Shearin, H.M.; Masson, P.H.; William, M. Resistivity of brine-saturated sands in relation to pore geometry. *Bull. Am. Assoc. Pet. Geol.* **1952**, *36*, 253–277.
46. Pirson, S.J. *Geologic Well Log Analysis*; Gulf Publishing: Houston, TX, USA, 1983.
47. Katsube, T.J. *Review of Formation Resistivity Factor Equations Related to New Pore-Structure Concepts*; Geological Survey of Canada: Ottawa, ON, Canada, 2010.
48. Ziarani, A.S.; Aguilera, R. Pore-throat radius and tortuosity estimation from formation resistivity data for tight-gas sandstone reservoirs. *J. Appl. Geophys.* **2012**, *83*, 65–73. [[CrossRef](#)]
49. Maxwell, J.C. *A Treatise on Electricity and Magnetism*, 3rd ed.; Clarendon Press Republished by Dover Publications, Inc.: New York, NY, USA, 1954.
50. Fricke, H. A mathematical treatment of the electric conductivity and capacity of disperse systems. *Phys. Rev.* **1924**, *24*, 575–587. [[CrossRef](#)]
51. Candelario, P.R. On the Relationship between Formation Resistivity Factor and Porosity. *Soc. Pet. Eng. J.* **1982**, *9*, 531–536.
52. Worthington, D.F. Improved Quantification of Fit for Purpose Saturation Exponents. *SPEE* **2004**, *7*, 270–284. [[CrossRef](#)]

Disclaimer/Publisher's Note: The statements, opinions and data contained in all publications are solely those of the individual author(s) and contributor(s) and not of MDPI and/or the editor(s). MDPI and/or the editor(s) disclaim responsibility for any injury to people or property resulting from any ideas, methods, instructions or products referred to in the content.